



*Supplement of*

## **Mechanistic insights into chloroacetic acid production from atmospheric multiphase volatile organic compound–chlorine chemistry**

**Mingxue Li et al.**

*Correspondence to:* Tao Wang (tao.wang@polyu.edu.hk)

The copyright of individual parts of the supplement might differ from the article licence.

This document includes Supplementary Tables S1-S4, and Supplementary Figures S1-S12.

### Table of contents

Table S1. Identified Cl-OVOCs and their precursors in previous VOC-Cl chamber experiments.

Table S2. Input data of the chemical box model for the campaign-averaged conditions.

Table S3. Branching ratios and rate constants of alkene + Cl<sup>•</sup> reactions.

Table S4. QC-calculated energies of solvation and aqueous-phase reactions of OVOCs and their reactive uptake coefficients.

Figure S1. The correlation coefficients between important meteorological factors and CAA concentration (a) during all day in 2020, (b) during all day in 2021, (c) during 10:00 – 14:00 in 2020 and (d) during 10:00 – 14:00 in 2021.

Figure S2. The primary reaction mechanisms of Cl<sup>•</sup> with 1-chloroethane (C<sub>2</sub>H<sub>5</sub>Cl), 1,2-dichloroethane (C<sub>2</sub>H<sub>4</sub>Cl<sub>2</sub>), 1,2-dichloropropane (C<sub>3</sub>H<sub>6</sub>Cl<sub>2</sub>), and ethene (C<sub>2</sub>H<sub>4</sub>).

Figure S3. Box model-simulated diurnal profiles of chloroacetic acid in different scenarios.

Figure S4. Relaxed scan of Cl<sup>•</sup> addition to isoprene.

Figure S5. Relaxed scan of Cl<sup>•</sup> addition to methacrolein (MACR).

Figure S6. Relaxed scan of Cl<sup>•</sup> addition to methyl vinyl ketone (MVK).

Figure S7. Proposed the primary reaction mechanisms of Cl<sup>•</sup> with propene (C<sub>3</sub>H<sub>6</sub>).

Figure S8. Proposed the primary reaction mechanisms of Cl<sup>•</sup> with isoprene (C<sub>5</sub>H<sub>8</sub>).

Figure S9. Proposed the primary reaction mechanisms of Cl<sup>•</sup> with methyl vinyl ketone (MVK).

Figure S10. Proposed the primary reaction mechanisms of Cl<sup>•</sup> with methacrolein (MACR).

Figure S11. Linear relationships between Gibbs free energy of diol reactions and reactive uptake coefficients of carbonyls.

Figure S12. Sensitivity testing of the effects of reactive uptake coefficients of Cl-OVOCs on simulated chloroacetic acid and Cl-OVOC levels using our updated model.

Table S1. Identified Cl-OVOCs and their precursors in previous VOC-Cl chamber experiments.

Cl-OVOCs	structure	precursor	structure	Ref.
		isoprene		(Orlando et al., 2003; Wennberg et al., 2018)
		methyl vinyl ketone		(Orlando et al., 2003)
		methacrolein		(Orlando et al., 2003)
formyl chloride		1,3-butadiene		(Orlando et al., 2003)
		1-butene		(Orlando et al., 2003)
		methyl acrylate		(Blanco et al., 2010)
		methyl 3-chloro-2-oxopropanoate		(Wennberg et al., 2018)
chloro-acetaldehyde		1-butene		(Orlando et al., 2003)
		acrolein		(Canosa-Mas et al., 2001)
		methyl vinyl ketone		(Canosa-Mas et al., 2001; Orlando et al., 2003)
		allyl alcohol		(Rodríguez et al., 2012)
		3-buten-2-ol		(Rodríguez et al., 2012)
		2-methyl-3-buten-2-ol		(Rodríguez et al., 2012)
		methacrolein		(Canosa-Mas et al., 2001; Kaiser et al., 2010; Orlando et al., 2003)
chloroacetone		2-methyl-2-propen-1-ol		(Rodríguez et al., 2012)
		3-methyl-3-buten-2-one		(Wang et al., 2015)

methyl 3-chloro-2-oxopropanoate		methyl acrylate		(Blanco et al., 2010)
3-chloro-4-hydroxy-2-butanone		crotyl alcohol		(Rodríguez et al., 2012)
2-chloro-propanal		crotyl alcohol		(Rodríguez et al., 2012)
4-chloro-crotonaldehyde		1,3-butadiene		(Orlando et al., 2003; Wang and Finlayson-Pitts, 2001)
chloro-methyl vinyl ketone		1,3-butadiene		(Wang and Finlayson-Pitts, 2001)
chloro-methylbutenal		isoprene		(Wennberg et al., 2018)
chloro-methylbutenone		isoprene		(Orlando et al., 2003; Wennberg et al., 2018)

Table S2. Input data of the chemical box model for the campaign-averaged conditions.

Parameter	Diurnal average <sup>a</sup>	Parameter	Diurnal average
T (K)	297.0 ± 1.0	propane (ppb)	1.0 ± 0.2
RH (%)	74.7 ± 5.0	isobutane (ppb)	0.39 ± 0.07
SO <sub>2</sub> (ppb)	2.7 ± 0.1	n-butane (ppb)	0.6 ± 0.1
CO (ppb)	264.8 ± 10.4	isopentane (ppb)	0.35 ± 0.07
NO (ppb)	0.33 ± 0.24	n-pentane (ppb)	0.23 ± 0.03
NO <sub>2</sub> (ppb)	3.2 ± 0.7	2-methylpentane (ppb)	0.36 ± 0.08
N <sub>2</sub> O <sub>5</sub> (ppb)	0.036 ± 0.029	n-hexane (ppb)	0.16 ± 0.05
HONO (ppb)	0.15 ± 0.03	cyclohexane (ppb)	0.022 ± 0.001
O <sub>3</sub> (ppb)	49.8 ± 9.9	acetylene (ppb)	1.3 ± 0.2
Sa (um <sup>2</sup> cm <sup>-3</sup> )	181.5 ± 23.2	ethene (ppb)	0.6 ± 0.1
ClNO <sub>2</sub> (ppb)	0.29 ± 0.23	propene (ppb)	0.10 ± 0.03
Cl <sub>2</sub> (ppb)	0.016 ± 0.014	isoprene (ppb)	0.17 ± 0.10
HOCl (ppb)	0.039 ± 0.019	α-pinene (ppb)	0.019 ± 0.007
BrCl (ppt)	0.64 ± 0.38	β-pinene (ppb)	0.010 ± 0.004
Br <sub>2</sub> (ppt)	3.1 ± 1.0	toluene (ppb)	0.36 ± 0.06
jNO <sub>2</sub> (10 <sup>-3</sup> s <sup>-1</sup> )	6.3 <sup>b</sup>	benzene (ppb)	0.15 ± 0.02
methane	2000 <sup>c</sup>	ethylbenzene (ppb)	0.05 ± 0.01
ethane (ppb)	1.7 ± 0.1	o-xylene (ppb)	0.04 ± 0.02

<sup>a</sup>Daily average ± standard deviation; <sup>b</sup>maximum value; <sup>c</sup>constant value.

Table S3. Branching ratios ( $\Gamma$ ) and rate constants ( $k$ ,  $10^{-10}$  cm<sup>3</sup>/molecule s) of alkene + Cl<sup>•</sup> reactions.

VOC	updated model			original model	
	$\Gamma$	$k$	Reference	$\Gamma$	$k$
C <sub>3</sub> H <sub>6</sub>	α-C addition: 92% abstraction: 8%	2.93	(Kaiser and Wallington, 1996)	α-C addition: 40% β-C addition: 50% abstraction: 10%	2.70
C <sub>5</sub> H <sub>8</sub>	α-C addition: 85% abstraction: 15%	4.75	(Wennberg et al., 2018)	addition: 100%	4.75
MVK	α-C addition: 75% abstraction: 25%	2.20	(Orlando et al., 2003)	-	2.20
MACR	α-C addition: 86% abstraction: 14%	2.30	(Sun et al., 2014)	-	1.70

Table S4. QC-calculated energies of solvation and aqueous-phase reactions of OVOCs and their reactive uptake coefficients<sup>1</sup>.

OVOC	$\Delta G_{\text{sol}}$	$\Delta G_{\text{hyd}}^{\ddagger}$	$\Delta_r G_{\text{hyd}}$	$\Delta G_{\text{sol}}^*$	$\lambda$	Ref.
formaldehyde	-1.30	41.84	0.17	-8.87	$2.00 \times 10^{-3}$	(Iraci and Tolbert, 1997)
glyoxal	-2.68	41.73	0.35	-11.13	$2.90 \times 10^{-3}$	(Liggio et al., 2005)
methylglyoxal	-3.30	42.75	1.80	-11.58	$3.70 \times 10^{-4}$	(De Haan et al., 2018)
2-butanone	-3.43	46.30	7.47	-7.62	$1.50 \times 10^{-4}$	(Schütze and Herrmann, 2004)
acetone	-3.55	47.84	7.93	-11.06	$1.80 \times 10^{-4}$	(Schütze and Herrmann, 2004)
2,3-butanedione	-3.78	45.74	5.41	-8.10	$8.00 \times 10^{-5}$	(Schütze and Herrmann, 2004)
formyl chloride	-1.14	28.79	-7.58	-9.04	$2.34 \times 10^{-2}$	this work
chloro-acetaldehyde	-3.42	42.31	1.87	-10.92	$8.23 \times 10^{-4}$	this work
chloro-acetone	-6.52	46.37	8.81	-8.40	$7.07 \times 10^{-5}$	this work
chloro-butanedione	-4.27	39.58	1.85	-8.55	$8.31 \times 10^{-4}$	this work
CMBO	-5.16	49.06	10.69	-10.13	$3.63 \times 10^{-5}$	this work
CAA	-	-	-	-	$7.05 \times 10^{-5}$	(Wang et al., 2020)

<sup>1</sup> $\Delta G_{\text{sol}}$  is solvation energy of OVOC,  $\Delta G_{\text{hyd}}^{\ddagger}$  and  $\Delta_r G_{\text{hyd}}$  are the Gibbs free energy changes between transition states and reactants and between products and reactants in the mono-hydration reactions of OVOC in the aqueous phase, respectively,  $\Delta G_{\text{sol}}^*$  is the evaporation energy of diol,  $\lambda$  is the reactive uptake coefficient from references and calculated in this work.

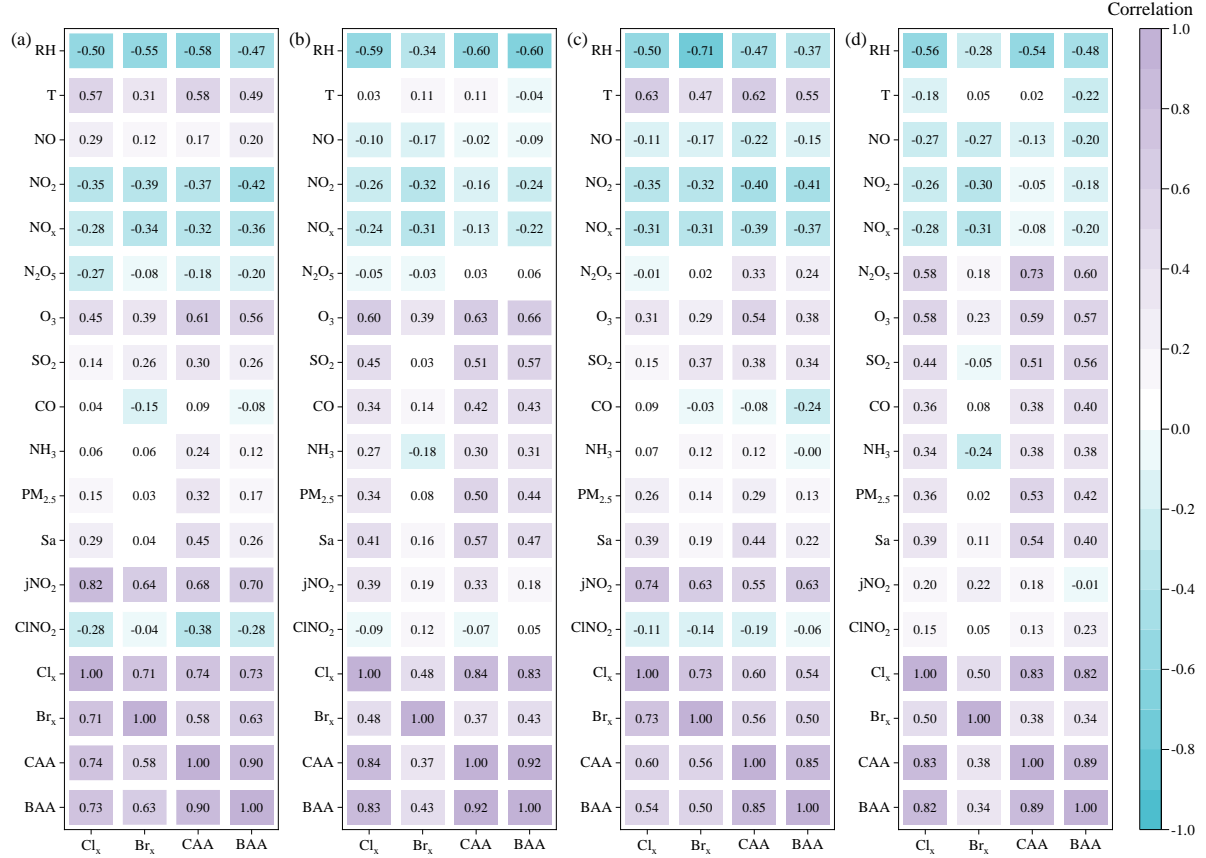


Figure S1. The correlation coefficients between important meteorological factors and CAA concentration (a) during all day in 2020, (b) during all day in 2021, (c) during 10:00 – 14:00 in 2020 and (d) during 10:00 – 14:00 in 2021.  $\text{Cl}_x = 2 \times \text{Cl}_2 + \text{HOCl} + \text{BrCl}$ , and  $\text{Br}_x = 2 \times \text{Br}_2 + \text{BrCl}$ . All data are 1-h averages.

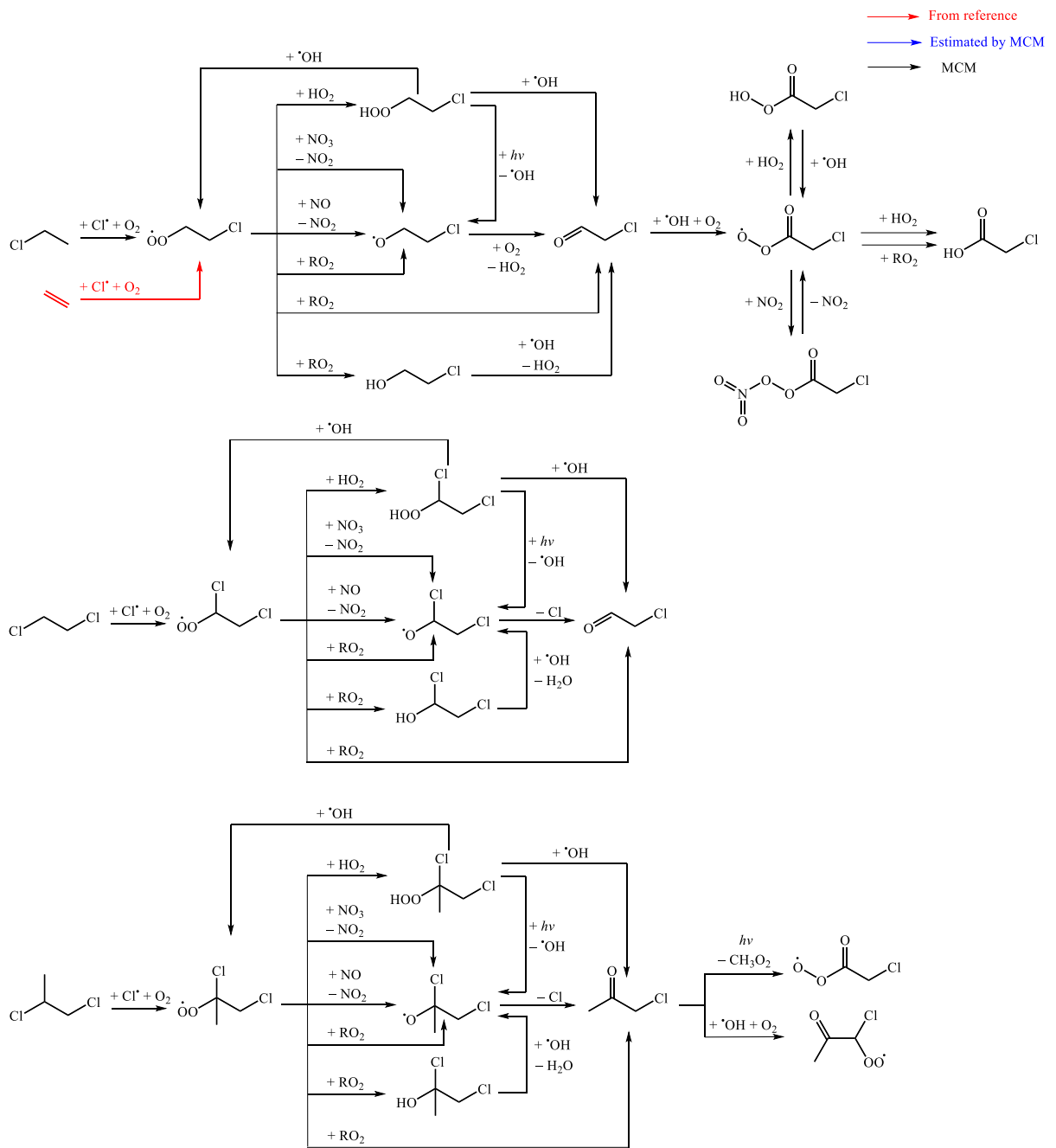


Figure S2. The primary reaction mechanisms of  $\text{Cl}\cdot$  with 1-chloroethane ( $\text{C}_2\text{H}_5\text{Cl}$ ), 1,2-dichloroethane ( $\text{C}_2\text{H}_4\text{Cl}_2$ ), 1,2-dichloropropane ( $\text{C}_3\text{H}_6\text{Cl}_2$ ), and ethene ( $\text{C}_2\text{H}_4$ ).

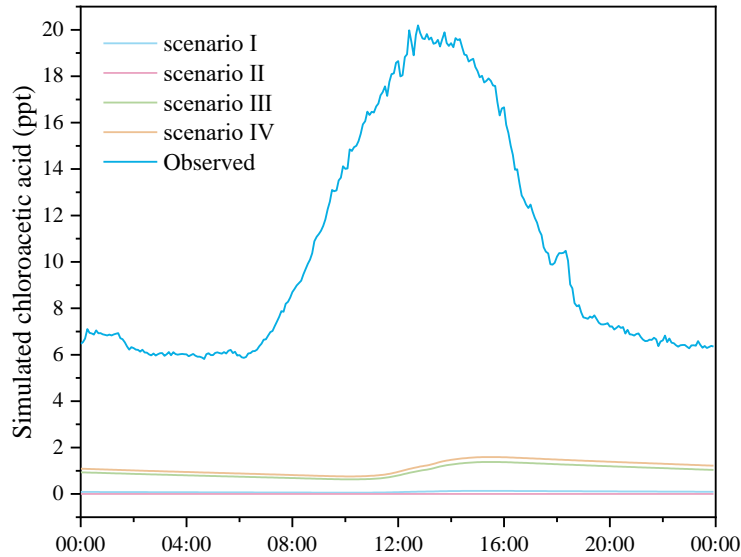


Figure S3. Box model-simulated and observed diurnal profiles of chloroacetic acid in different scenarios. The simulated result of scenario II is close to zero.

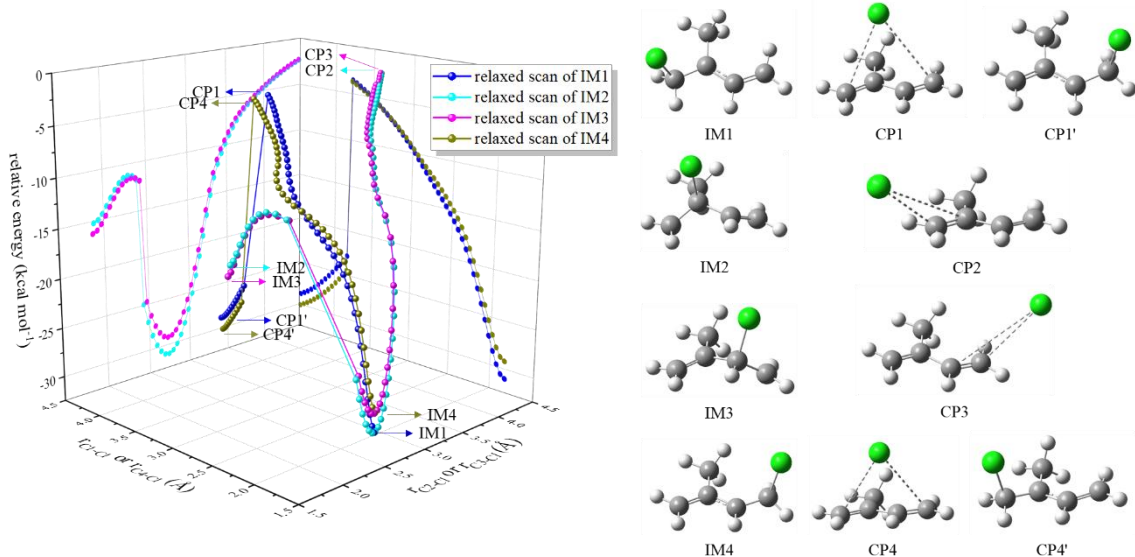


Figure S4. Relaxed scan of  $\text{Cl}\cdot$  addition to isoprene. IM1, IM2, IM3, and IM4 are intermediates for  $\text{Cl}\cdot$  addition to 1-, 2-, 3-, and 4-positions of isoprene, and CP1 – CP4, CP1' and CP4' are derived from scans of IM1 – IM2 in terms of bond lengths ( $r$ ) of C-Cl as variables, respectively. Scanned potential energy surfaces of IM1 – IM4 take the total energy of the reactants  $\text{Cl}\cdot + \text{isoprene}$  as zero for reference. The relative energies of IM1 and IM4 are lowest. A relaxed scan of IM1 reveals a minimum energy path (MEP):  $\text{CP1}' \leftarrow \text{CP1} \leftarrow \text{IM1}$ , where CP1' approximates IM4. The relaxed scan of IM4 also reveals interconversion between IM1 and IM4, but the energy barriers are too high to be difficult to occur. The relaxed scans of IM2 and IM3 reveal the MEP of  $\text{IM2} \leftarrow \text{IM1} \leftarrow \text{CP2}$  and  $\text{IM3} \leftarrow \text{IM4} \leftarrow \text{CP3}$ . Saddle points of IM2 and IM3 are difficult to reach due to their conversion to IM1 and IM4 passing through low-energy barriers. Thus,  $\text{Cl}\cdot$  prefers to add to 1- and 4-positions of isoprene.

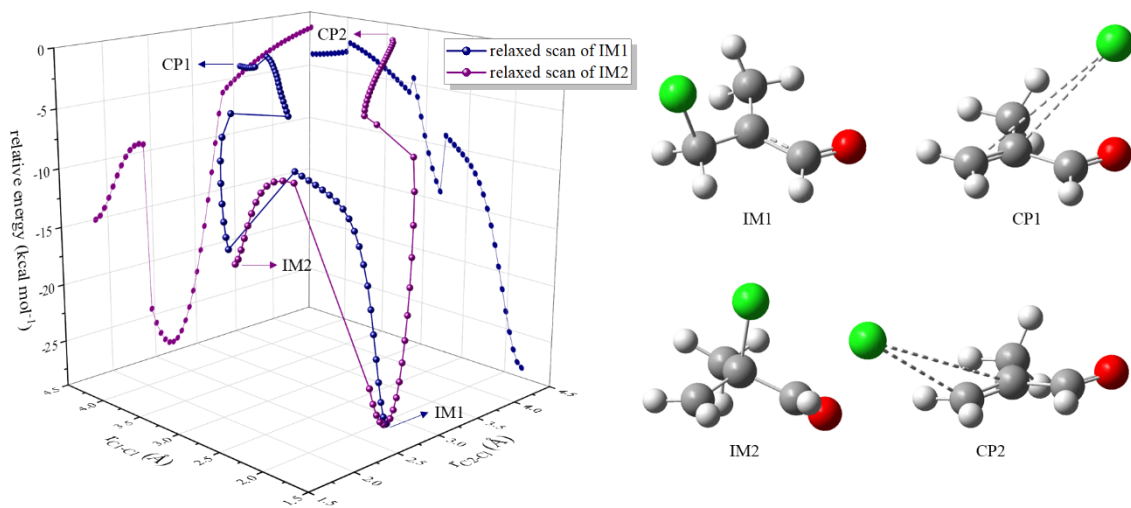


Figure S5. Relaxed scan of Cl<sup>·</sup> addition to methacrolein (MACR). Similar to the Cl<sup>·</sup> addition of propene.

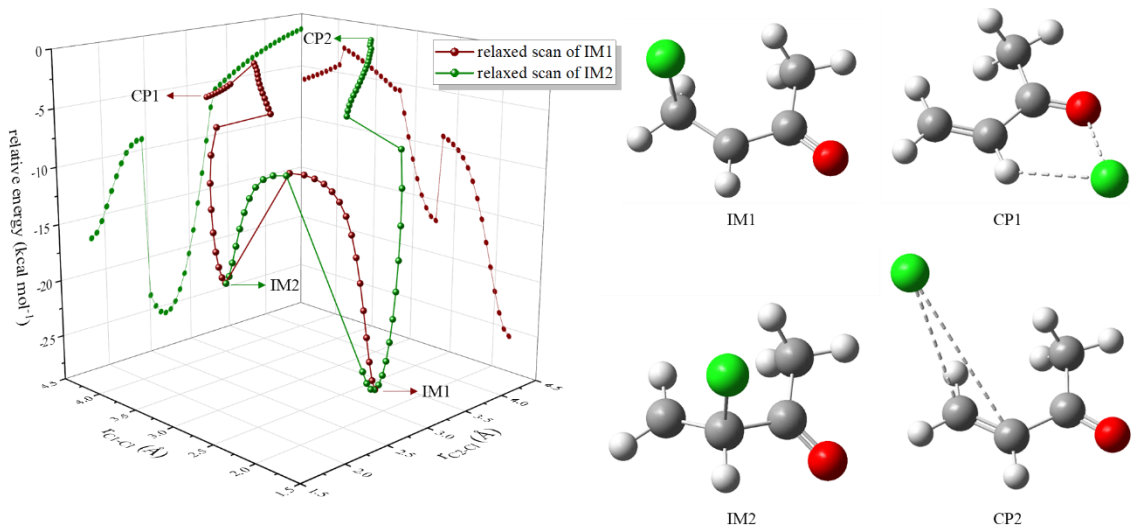


Figure S6. Relaxed scan of Cl<sup>·</sup> addition to methyl vinyl ketone (MVK). Similar to the Cl<sup>·</sup> addition of propene.

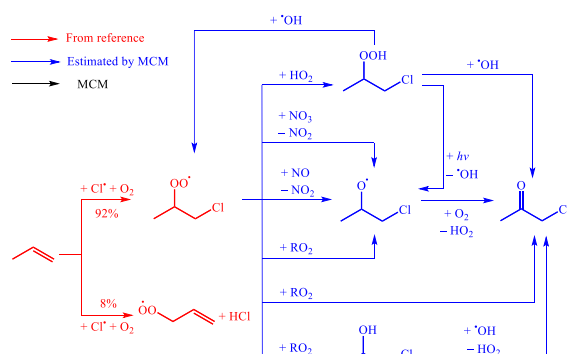


Figure S7. Proposed the primary reaction mechanisms of Cl<sup>·</sup> with propene (C<sub>3</sub>H<sub>6</sub>).

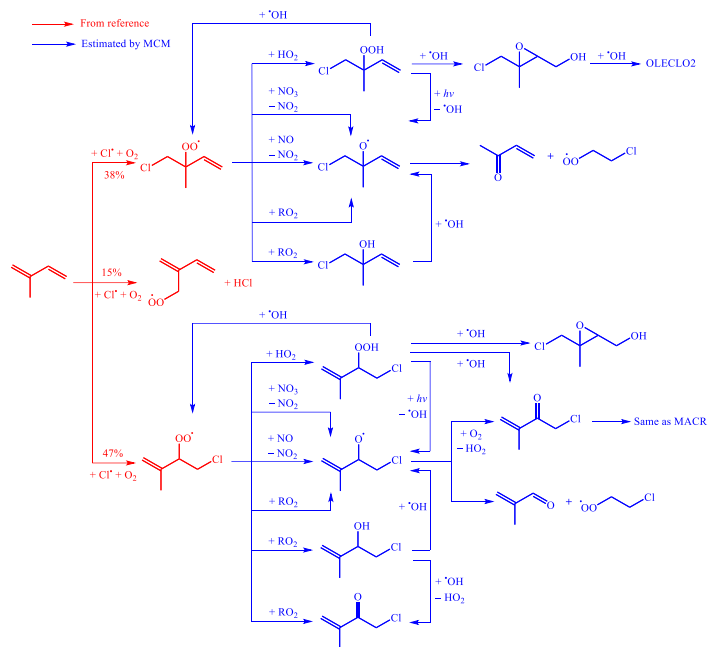


Figure S8. Proposed the primary reaction mechanisms of  $\text{Cl}^*$  with isoprene ( $\text{C}_5\text{H}_8$ ).

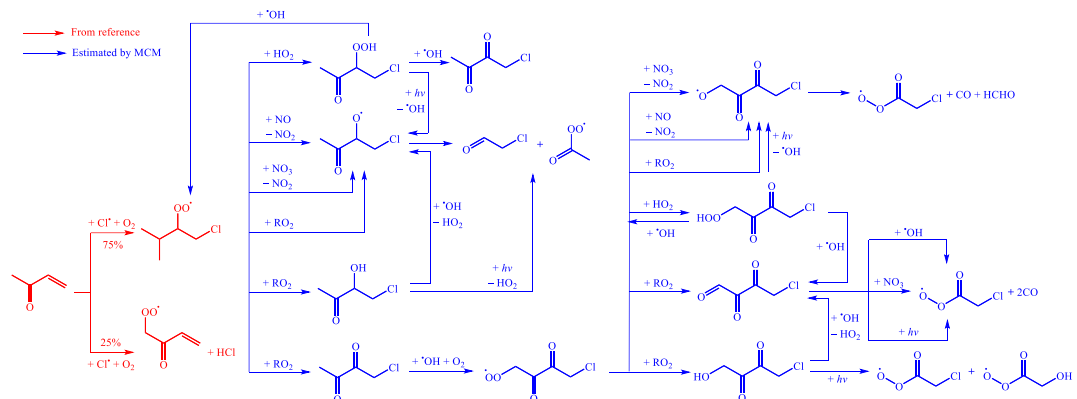


Figure S9. Proposed the primary reaction mechanisms of  $\text{Cl}^*$  with methyl vinyl ketone (MVK).

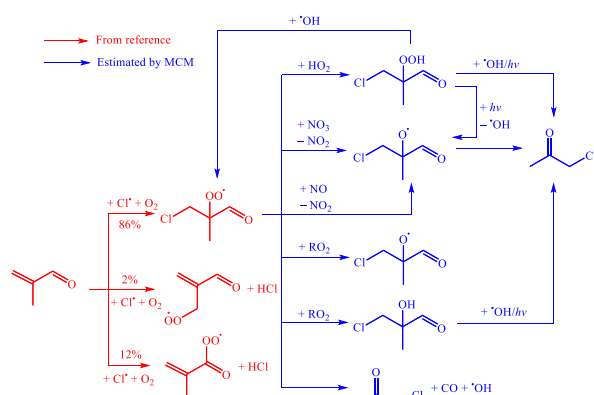


Figure S10. Proposed the primary reaction mechanisms of  $\text{Cl}^*$  with methacrolein (MACR).

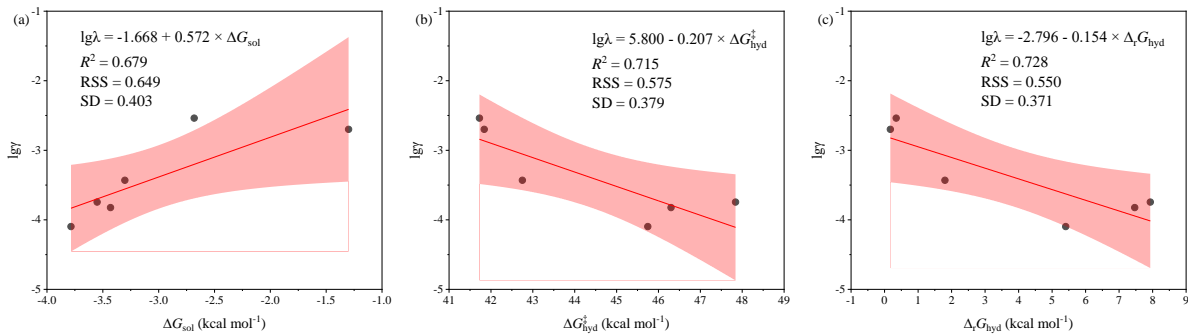


Figure S11. Linear relationships between Gibbs free energy of diol reactions and reactive uptake coefficients of carbonyls. (a)  $\Delta G_{\text{sol}}$  as the solvation energy of carbonyls; (b)  $\Delta G_{\text{hyd}}^+$  and (c)  $\Delta_r G_{\text{hyd}}$  as the Gibbs free energy barriers and changes in the hydration reactions of carbonyls;  $\lambda$  as the reactive uptake coefficients;  $R^2$  as the coefficient of determination; RSS as the residual sum of squares; SD as the standard deviation.

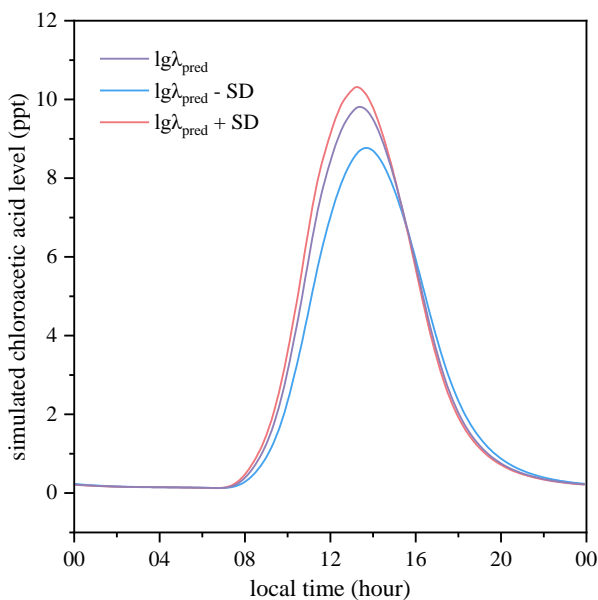


Figure S12. Sensitivity testing of the effects of reactive uptake coefficients of Cl-OVOCs on simulated chloroacetic acid and Cl-OVOC levels using our updated model.  $\lambda_{\text{pred}}$  are the predicted reactive uptake coefficients of Cl-OVOCs according to the linear relationship model between  $\Delta_r G_{\text{hyd}}$  and  $\lg\lambda$ , and SD is the standard deviation.

## Reference

- Blanco, M. B., Bejan, I., Barnes, I., Wiesen, P., and Teruel, M. A.: FTIR product distribution study of the Cl and OH initiated degradation of methyl acrylate at atmospheric pressure, *Environ. Sci. Technol.*, 44, 7031–7036, <https://doi.org/10.1021/es101831r>, 2010.
- Canosa-Mas, C. E., Cotter, E. S. N., Duffy, J., Thompson, K. C., and Wayne, R. P.: The reactions of atomic chlorine with acrolein, methacrolein and methyl vinyl ketone, *Phys. Chem. Chem. Phys.*, 3, 3075–3084, <https://doi.org/10.1039/b101434j>, 2001.
- De Haan, D. O., Jimenez, N. G., De Loera, A., Cazaunau, M., Gratien, A., Pangui, E., and Doussin, J.-F.: Methylglyoxal uptake coefficients on aqueous aerosol surfaces, *J. Phys. Chem. A*, 122, 4854–4860, <https://doi.org/10.1021/acs.jpca.8b00533>, 2018.
- Iraci, L. T. and Tolbert, M. A.: Heterogeneous interaction of formaldehyde with cold sulfuric acid: Implications for the upper troposphere and lower stratosphere, *J. Geophys. Res.*, 102, 16099–16107, <https://doi.org/10.1029/97JD01259>, 1997.
- Kaiser, E. W. and Wallington, T. J.: Pressure Dependence of the Reaction Cl + C<sub>3</sub>H<sub>6</sub>, *J. Phys. Chem.*, 100, 9788–9793, <https://doi.org/10.1021/jp960406r>, 1996.

- Kaiser, E. W., Pala, I. R., and Wallington, T. J.: Kinetics and mechanism of the reaction of methacrolein with chlorine atoms in 1–950 Torr of N<sub>2</sub> or N<sub>2</sub>/O<sub>2</sub> diluent at 297 K, *J. Phys. Chem. A*, 114, 6850–6860, <https://doi.org/10.1021/jp103317c>, 2010.
- Liggio, J., Li, S., and McLaren, R.: Reactive uptake of glyoxal by particulate matter, *J. Geophys. Res.*, 110, 2004JD005113, <https://doi.org/10.1029/2004JD005113>, 2005.
- Orlando, J. J., Tyndall, G. S., Apel, E. C., Riemer, D. D., and Paulson, S. E.: Rate coefficients and mechanisms of the reaction of Cl-atoms with a series of unsaturated hydrocarbons under atmospheric conditions, *Int. J. Chem. Kinet.*, 35, 334–353, <https://doi.org/10.1002/kin.10135>, 2003.
- Rodríguez, A., Rodríguez, D., Soto, A., Bravo, I., Diaz-de-Mera, Y., Notario, A., and Aranda, A.: Products and mechanism of the reaction of Cl atoms with unsaturated alcohols, *Atmos. Environ.*, 50, 214–224, <https://doi.org/10.1016/j.atmosenv.2011.12.030>, 2012.
- Schütze, M. and Herrmann, H.: Uptake of acetone, 2-butanone, 2,3-butanedione and 2-oxopropanal on a water surface, *Phys. Chem. Chem. Phys.*, 6, 965–971, <https://doi.org/10.1039/B313474A>, 2004.
- Sun, C., Xu, B., and Zhang, S.: Atmospheric reaction of Cl + methacrolein: A theoretical study on the mechanism, and pressure- and temperature-dependent rate constants, *J. Phys. Chem. A*, 118, 3541–3551, <https://doi.org/10.1021/jp500993k>, 2014.
- Wang, J., Zhou, L., Wang, W., and Ge, M.: Gas-phase reaction of two unsaturated ketones with atomic Cl and O<sub>3</sub>: kinetics and products, *Phys. Chem. Chem. Phys.*, 17, 12000–12012, <https://doi.org/10.1039/C4CP05461J>, 2015.
- Wang, W. and Finlayson-Pitts, B. J.: Unique markers of chlorine atom chemistry in coastal urban areas: The reaction with 1,3-butadiene in air at room temperature, *J. Geophys. Res.*, 106, 4939–4958, <https://doi.org/10.1029/2000JD900683>, 2001.
- Wang, Y., Zhou, L., Wang, W., and Ge, M.: Heterogeneous uptake of formic acid and acetic acid on mineral dust and coal fly ash, *ACS Earth Space Chem.*, 4, 202–210, <https://doi.org/10.1021/acsearthspacechem.9b00263>, 2020.
- Wennberg, P. O., Bates, K. H., Crounse, J. D., Dodson, L. G., McVay, R. C., Mertens, L. A., Nguyen, T. B., Praske, E., Schwantes, R. H., Smarte, M. D., St Clair, J. M., Teng, A. P., Zhang, X., and Seinfeld, J. H.: Gas-phase reactions of isoprene and its major oxidation products, *Chem. Rev.*, 118, 3337–3390, <https://doi.org/10.1021/acs.chemrev.7b00439>, 2018.